Glass-bearing xenoliths from Cape Verde: Evidence for a hot rising mantle jet

Article *in* Mineralogy and Petrology · December 1995

DOI: 10.1007/BF01165119

4 authors, including:

T. Ntaflos
University of Vienna
495 PUBLICATIONS **3,212** CITATIONS

SEE PROFILE

Lia Kogarko
Russian Academy of Sciences
246 PUBLICATIONS **2,447** CITATIONS

SEE PROFILE

Mineralogy and Petrology (1995) 55: 217–237

Mineralogy and Petrology

Glass-bearing xenoliths from Cape Verde: evidence for a hot rising mantle jet

I. D. Ryabchikov[1], **T. Ntaflos**[2], **G. Kurat**[3], and **L. N. Kogarko**[4]

[1] Institute for Geology of Ore Deposits, Russian Academy of Sciences, Moscow, Russia
[2] Institute of Petrology, University of Vienna, Austria
[3] Naturhistorisches Museum, Wien, Austria
[4] Vernadsky Institute of Geochemistry, Russian Academy of Sciences, Moscow, Russia

With 2 Figures

Received April 12, 1994;
accepted October 27, 1994

Summary

Peridotitic xenoliths from melanephelinites of Sal Island, Cape Verde Archipelago, have a compositional range from moderately depleted lherzolites to refractory harzburgites. Most xenoliths have protogranular textures but porphyroclastic and mylonitic textures are not uncommon. Small amounts of glass are present in the intergranular space of these rocks which possibly, at least in part, represent quenched silicate melt which invaded these rocks just before they were excavated. These glasses contain microphenocrysts of olivine, clinopyroxene, and spinel, as well as small grains of sulphides and metallic Fe-Ni alloys. Metallic phases were most likely produced by the desulphurization of sulfides, which also resulted in very low oxygen fugacities (several logarithmic units below QFM buffer) in the interstitial glasses and associated microphenocrysts. This is reflected in the chemical composition of the newly formed spinels which are characterised by low amounts of ferric iron. In contrast, primary spinel-bearing mineral assemblages of the peridotites were formed at much higher f_{O_2}, which were similar to those estimated for the host nephelinites which have high titanomagnetite contents.

Zusammenfassung

Glasführende Xenolithe von Kap Verde: Evidenz für einen heißen Erdmantel Diapir

Die ultramafischen Xenolithe aus den Melanepheliniten von der Kap Verde Insel Sal sind Spinell-Lherzolithe und Spinell-Harzburgite. Am verbreitesten sind Xenolithe mit protogranularer Textur, aber auch Xenolithe mit porphyroklastischer und mylonitischer Textur treten häufig auf. Die Xenolithe enthalten kleine Mengen von intergranularem Glas, welches, wenigstens zum Teil, abgeschreckte silikatische Schmelzen repräsentiert,

welche die Gesteine vor ihrem Aufstieg aus dem Erdmantel durchdrungen haben. Dieses Glas enthält Mikrophenokristalle von Olivin, Klinopyroxen und Orthopyroxen, sowie auch kleinere Körner von Sulfiden und metallischen Fe-Ni Legierungen. Metallische Phasen sind sehr wahrscheinlich durch Entschwefelung von Sulfiden unter sehr niedrigem f_{O2} (einige Größenordnungen unter dem QFM Buffer) entstanden. Das wirkt sich auf die Zusammensetzung der neu gebildeten Spinelle aus, die durch einen niederen Gehalt an Fe^{3+} charakterisiert sind. Die Xenolithe wurden jedoch unter viel höhere f_{O2} gebildet. Ihre f_{O2} sind ähnlich der für die Wirtsnephelinite berechneten f_{O2}, die hohe Titanomagnetit-Gehalte aufweisen.

Introduction

Mantle xenoliths containing glasses were described by a number of investigators from a variety of locations (*Edgar* et al., 1989; *Kleeman* et al., 1969; *Ellis*, 1976; *Francis*, 1992; *Frey* and *Green*, 1974; *Gamble* and *Kyle*, 1987; *Garcia* and *Presti*, 1987; *Siena* et al., 1991; *Schiano* et al., 1992). Glasses have been found to occur in veins, in patches, as intergranular films and very commonly, as inclusions in olivine, clinopyroxene and spinel. A wide variety of chemical compositions has been reported ranging from high silica (~65 wt %) to low silica (~35 wt%), from high alkali (~15 wt% $Na_2O + K_2O$) to low alkali (~4 wt% $Na_2O + K_2O$), low alumina (0.1 wt% Al_2O_3) to high alumina (23 wt% Al_2O_3), etc. A wide spectrum of opinions exists concerning the origin and significance of such glasses. It has been proposed that they may represent incipient melts produced by decompression as mantle rocks were transported to the surface (*Kuo* and *Essene*, 1986), or that they result from infiltration of host magma into the xenoliths (*Caperdi* et al., 1989), or that they are samples of melts responsible for mantle metasomatism at depth (*Siena* and *Coltori*, 1993). It has also been argued, that xenolith glasses reflect the chemistry of primary magmas, which may be produced by partial melting of various types of mantle rocks (*Francis*, 1991).

This paper examines the interstitial glasses of mantle xenoliths collected at Cape Verde Islands, their relations with associated microphenocrysts, host basalts and primary minerals of mantle rocks. Particular emphasis was put on estimating oxygen fugacities in the mantle based upon the composition of coexisting phases in these rocks.

Samples and methods

About 100 upper mantle xenoliths were collected in 1985 by one of us (LNK) on Sal Island, Cape Verde Archipelago, during a four months geological expedition organized by the Academy of Sciences of the Soviet Union. These xenoliths occur in olivine melanephelinites of the Morro do Aquar volcanic system (neovolcanic complex). Upper mantle xenoliths have previously been described from several islands of the Cape Verde Archipelago (*De Paepe* and *Klerkx*, 1971; *Mendes* and *Silva*, 1983; *Siena* and *Coltari*, 1993). Rock types encountered include lherzolites and harzburgites containing primary phlogopite and xenoliths rich in fluid inclusions. On Sal Island mostly strongly tectonized samples are found with porphyroclastic and mylonitic textures. We selected 10 glass-bearing samples representing the most common rock types (lherzolite to harzburgite) and the most common textural types.

Mantle rocks and host nephelinites were investigated by optical microscopy and scanning electron microscopy. Phase analyses were performed by an EDX-KEVEX system attached to an JEOL-6400 scanning electron microscope (Mineralogisch-Petrographische Abteilung, Naturhistorisches Museum, Vienna). Critical data were collected by utilising an ARL SEMQ electron microprobe with five wavelength-dispersive spectrometers (Institut für Petrologie, University of Vienna). Measurements were made at 15 kV and 20 nA against well defined standards and were corrected for matrix effect by the ZAF method (*Armstrong*, 1988).

Olivines and other primary minerals from four lherzolites (CV-5, CV-8, CV-17 and CV-55) and one harzburgite (CV-1) were analysed for their calcium contents by electron microprobe with wavelength dispersive spectrometers employing extended counting times and comparing the count data to those acquired on San Carlos olivine as recommended by *Köhler* and *Brey* (1990).

Sample description

A routine inspection of the samples collected revealed the presence of a surprisingly large number of peridotitic xenoliths containing interstitial glass. The ten samples collected are believed to be representative of the variety encountered. Their main petrographic features are listed in Table 1. The rocks selected are spinel lherzolites and spinel harzburgites. In one sample (CV-8) no primary spinel has been found. Textures are mainly protogranular (according to the terminology of *Mercier* and *Nicolas*, 1975), but secondary protogranular and transitional textures between protogranular and porphyroclastic are also present (Table 1). Only one sample, CV-37, has a mosaic equigranular texture with relics of coarse-grained and strongly deformed porphyroclasts. Minerals of rocks with protogranular textures are generally not deformed. Olivine is coarse-grained (up to 2.4 mm), occasionaly weakly kinkbanded and lacks mineral inclusions. However, abundant secondary gas-filled fluid microinclusions are commonly found in olivines along zones intersecting the rocks. The secondary protogranular texture differs from the primary protogranular in that large olivine and orthopyroxene grains contain fine-grained (up to 0.30 mm in diameter) inclusions of rounded spinel. In contrast, spinels in spinel lherzolites are always associated with clinopyroxene and orthopyroxene. The colour of spinels varies between green- and red-brownish in spinel lherzolites and brown in spinel harzburgites. Sample CV-37 (Table 1) with mosaic equigranular texture is unusually rich in spinel (ca 8 wt%) and contains relictic porphyroclasts of olivine and orthopyroxene which are strongly deformed. In CV-37 rounded grains of brown spinel up to 1.2 mm in diameter occur at triple junctions and smaller grains as inclusions in the porphyroclasts. In spinel lherzolites clinopyroxene and orthopyroxene are always smaller than olivine and do not contain exsolution lamellae. However, in spinel harzburgites some orthopyroxenes show very thin exsolution lamellae.

A very characteristic feature of the Sal Island xenoliths is the presence of glass which occurs mainly in the intergranular space of these rocks or as small inclusions in olivine and orthopyroxene. Where glass is in contact with clinopyroxene and/or spinel, reactions are apparent: a spongeous belt of reaction products, up to 0.2 mm wide, developed, consisting of olivine and clinopyroxene microphenocrysts, vermicular brown spinel, sulfides and spherules of sulfides with metallic Fe-Ni exsolutions or euhedral Fe-Ni metal grains, all embedded in a glassy matrix. Melt patches with the same spongeous texture are also found at triple junctions. Small inclusions of melt, sulfides and metallic Fe-Ni are found mainly in olivine and orthopyroxene in form of purple strings along cracks. Spinel lherzolites are generally richer in sulfides and Fe-Ni metal than harzburgites. Two of the ten samples, CV-37 and CV-55, are unusually rich in sulfides and metallic Fe-Ni alloy.

Table 1. *Petrographic features of Cape Verde xenoliths*

Sample	Rock type	Texture	Modal mineral composition in wt%*
CV-1	spinel harzburgite	transitional; protogranular to porphyroclastic	
CV-4	spinel harzburgite	protogranular	
CV-5	spinel lherzolite	secondary protogranular	0l = 47.9, opx = 29.9, cpx = 20.1, sp = 1.0
CV-6	spinel harzburgite	protogranular	
CV-7	spinel lherzolite	protogranular	ol = 65.4, opx = 27.7, cpx = 4.8, sp = 1.7
CV-8	lherzolite	protogranular	
CV-17	spinel lherzolite	transitional; protogranular to porphyroclastic	ol = 68.5, opx = 19.7, cpx = 10.6, sp = 0.8
CV-37	spinel lherzolite	mosaic equigranular	
CV-55	spinel lherzolite	protogranular	ol = 65.1, opx = 18.6, cpx = 13.7, sp = 2.1
CV-69	spinel harzburgite	secondary protogranular	ol = 81.8, opx = 14.8, cpx = 1.7, sp = 0.8

* Modal mineral composition were calculated from microprobe analyses of primary minerals and bulk compositions (*Kogarko* 1990)

Table 2. *WDS and EDS electron microprobe analyses of olivine in peridotitic xenoliths from Cape Verde Islands (in wt%)*

Sample	CV-1	CV-1	CV-4	CV-5	CV-6	CV-7	CV-8	CV-8	CV-17	CV-17	CV-37	CV-37	CV-55	CV-55	CV-69	CV-69
	#	#s		#			#	#s	#	s		s	#	s	#	#s
SiO_2	41.5	40.8	41.6	41.3	41.9	41.2	41.6	42.0	41.1	40.1	40.6	40.5	41.2	40.5	40.9	41.0
Cr_2O_3	<0.02	0.02	0.07	0.07	0.16	0.10	0.10	0.20	0.06	0.27	0.14	0.40	0.08	0.40	<0.02	0.06
FeO*	8.0	7.7	7.5	8.3	7.4	8.4	8.8	8.8	9.1	9.4	11.7	12.4	9.8	9.4	8.0	7.5
MnO	0.14	0.11	0.18	0.14	0.08	0.09	0.12	0.09	0.12	0.10	0.12	0.11	0.13	0.11	0.14	0.08
NiO	0.36	0.15	0.41	0.25	0.40	0.32	0.38	0.23	0.32	0.15	0.37	0.28	0.36	0.22	0.34	0.24
MgO	50.6	49.9	50.2	49.8	49.9	48.7	49.6	49.8	49.1	49.2	46.4	46.0	48.4	48.8	50.0	50.1
CaO	0.04	0.22	0.12	0.17	0.12	0.22	0.16	0.20	0.15	0.21	0.28	0.17	0.17	0.22	0.11	0.18
Total	100.64	98.90	100.00	99.99	99.88	98.92	100.75	101.23	99.98	99.46	99.57	99.89	100.09	99.64	99.49	99.18
mg	91.6	91.9	92.3	91.4	92.3	91.2	90.8	91.0	91.0	90.3	87.6	86.8	91.1	90.3	91.6	92.2

s olivine microphenocrysts in interstitial glass. *Total Fe as FeO; # WDS analyses

Table 3. *WDS and EDS electron microprobe analyses of orthopyroxene in peridotitic xenoliths from Cape Verde Islands (in wt%)*

Sample	CV-1	CV-4	CV-5	CV-6	CV-7	CV-8	CV-17	CV-37	CV-55	CV-69
	#		#			#	#		#	
SiO_2	58.2	56.3	55.1	55.7	54.9	54.8	54.3	53.8	54.1	56.8
TiO_2	<0.02	0.10	0.10	0.10	0.23	0.11	0.31	0.30	0.21	0.06
Al_2O_3	1.89	3.2	4.4	2.9	4.8	5.5	5.4	5.9	6.1	3.2
Cr_2O_3	0.71	0.70	1.03	0.65	0.80	1.29	0.88	0.49	0.58	0.58
FeO*	5.3	5.2	5.3	4.8	5.1	5.6	5.8	6.7	6.0	4.8
MnO	0.16	0.04	0.11	0.11	0.05	0.06	0.10	0.05	0.12	0.08
NiO	0.07	0.13	0.10	0.09	0.11	0.11	0.12	0.13	0.08	0.07
MgO	34.6	33.1	32.3	34.0	32.5	31.6	31.4	31.2	31.1	32.9
CaO	0.70	1.35	1.57	1.55	1.51	1.67	1.56	1.38	1.57	1.67
Na_2O	0.02	<0.02	0.10	0.02	<0.02	0.08	0.16	<0.02	0.21	<0.02
Total	101.62	100.00	100.00	99.86	99.97	100.81	100.01	99.84	100.00	100.08
mg	91.8	92.0	91.6	92.7	91.9	91.0	90.0	89.3	90.3	92.4

* Total Fe as FeO; # WDS analyses

Chemical analyses of minerals of the peridotites are given in Tables 2–5. In the least refractory rocks the Mg/(Mg + Fe) atomic ratio of olivine (henceforth called Mg-number, mg) is close to 0.88. Orthopyroxene, clinopyroxene and spinel of these rocks are characterised by high alumina contents, and the Na_2O content of clinopyroxene exceeds 1 wt%. In some harzburgites the mg of olivines reaches 0.92 and for clinopyroxene 0.95. Orthopyroxene and clinopyroxene in these rocks are less aluminous, the sodium content in primary clinopyroxene is low, and primary spinels are richer in Cr as compared to lherzolites.

Interstitial glasses in the xenoliths are in the majority of cases characterised by high Na, K and Al contents, SiO_2 contents close to 60 wt%, and low Mg, Ca and Fe contents (Table 6). They also have high Ni/Fe ratios. Glasses rich in Mg and Al and poor in alkalies are rarer. Both types of glasses can be present in one xenolith. Alkali-rich glasses are much more common in lherzolites than in harzburgites.

Alkali-rich interstitial glasses typically contain microphenocrysts of olivine, clinopyroxene and spinel, but no orthopyroxene (Fig. 1A). Glasses of samples CV-4 and CV-8 in addition contain rare microphenocrysts of apatite. Occasionally, relics of orthopyroxene surrounded by rims of clinopyroxene can be present in the glass. Olivine microphenocrysts are similar in major element composition to the primary peridotitic olivines, but characterized by higher Cr contents and lower Ni as compared to the latter. Secondary clinopyroxenes and spinels have much lower Al contents as compared to their primary counterparts (Tables 4 and 5). Ratios of Fe^{3+}/Fe^{2+}, calculated on the assumption of perfect stoichiometry for secondary spinels are also in the majority of cases significantly lower than for primary spinel from the same specimen. Primary and newly formed spinels fall into separate fields in the plane $Mg/(Mg + Fe) - Cr/(Cr + Al + Fe^{3+})$, with the exception of secondary spinels from samples CV-5 and CV-8 which plot near the Cr-rich boundary of the primary spinel field (Fig. 2). For lherzolitic nodules sodium concentrations in clinopyroxenes included in glass are also much lower than in clinopyroxenes of the peridotite. Large primary clinopyroxenes in contact with glass change composition towards that of secondary clinopyroxenes (decreasing Na and Al), with the central parts remaining unchanged. A gradual change in composition away from the contact with glass is developed in such cases. Similar zoning is present in primary spinels in contact with quenched melt. The marginal parts of such spinels are corroded.

Sulfides are rare outside melt pockets but occasionally small grains are present at silicate grain-boundaries. In contrast, the interstitial glass commonly contains sulfide aggregates. Sulfides usually have irregular rounded shapes reminescent of a sulfide liquid immiscible with silicate melt (Fig. 1B). The most common sulfide is a monosulfide solid solution containing from <2 to 46 wt% Ni and between <0.02 and 5 wt% Cu (Table 7). The Ni-poor sulfides are most widespread. In addition to the monosulfides a Ni-rich $Ni_{3+x}S_2$ phase is present. This phase commonly contains metal inclusions. Metallic alloys are more common in lherzolites than in harzburgites.

Metallic phases vary in composition from <1 to 67 wt% Ni and <1 to 2 wt% Cu. In many cases large variations are observed even within one specimen. Lherzolite CV-55 differs from other peridotites in having metallic segregations of rather constant composition close to Ni_2Fe, forming sometimes euhedral grains (Fig. 1c) without associated sulfides. In this rock metal is much more abundant than sulfides which are Fe-poor $Ni_{3+x}S_2$. Occasionally these sulfides form thin coatings on the metal grains.

The volcanic host rock of the xenoliths is a melanephelinite consisting of several generations of phenocrysts and microphenocrysts in a glassy matrix. The earliest generation are olivine phenocrysts (Fo_{86}) with high CaO contents (about 1 wt%). The space between olivines is filled mainly by microphenocrysts of clinopyroxene and titanomagnetite. The latest generation of microphenocrysts is represented by apatite and rare amphibole. Residual

Table 4. *WDS and EDS electron microprobe analyses of clinopyroxene in peridotitic xenoliths from Cape Verde Islands (in wt%)*

Sample	CV-1 #	CV-1 #s	CV-4	CV-4 s	CV-5 #	CV-5 #s	CV-6	CV-6 s	CV-7	CV-7 s
SiO_2	54.5	55.3	53.4	55.1	52.4	52.8	53.3	54.8	53.3	54.8
TiO_2	<0.02	0.04	0.18	0.18	0.27	0.73	0.14	0.23	0.14	0.23
Al_2O_3	2.03	0.47	2.08	0.61	5.3	1.81	2.41	0.88	2.41	0.88
Cr_2O_3	0.96	1.86	0.72	1.64	1.33	1.33	0.86	1.26	0.86	1.26
FeO*	2.08	2.50	1.50	2.27	3.4	2.9	2.30	2.7	2.30	2.7
MnO	0.09	<0.02	0.12	0.05	0.10	0.21	0.08	0.03	0.08	0.03
NiO	0.04	0.03	0.08	0.08	0.09	0.31	0.21	0.19	0.21	0.19
MgO	17.8	19.1	17.5	19.4	18.0	19.5	19.2	19.5	19.2	19.5
CaO	23.5	20.7	24.3	20.2	18.5	20.1	21.6	20.2	21.6	20.2
Na_2O	0.04	0.77	0.14	0.52	0.58	0.30	<0.02	0.26	<0.02	0.26
Total	101.08	100.74	99.95	100.00	100.00	100.00	100.07	100.00	100.07	100.00
mg	94.3	94.2	95.4	92.3	90.5	92.4	93.7	92.8	93.7	92.8

Sample	CV-8 #	CV-8 #s	CV-17 #	CV-17 #s	CV-37	CV-55 #	CV-55 #s	CV-69	CV-69 s
SiO_2	52.6	54.8	51.9	53.6	51.2	51.6	53.2	53.0	55.0
TiO_2	0.37	0.20	0.72	0.51	0.69	0.60	0.71	0.20	0.18
Al_2O_3	6.5	1.01	6.5	2.21	6.7	7.3	1.97	2.6	0.58
Cr_2O_3	1.82	1.71	1.3	1.29	1.08	0.89	1.16	0.81	1.67
FeO*	3.5	2.27	3.7	2.7	4.6	3.9	2.41	1.92	2.36
MnO	0.09	0.07	0.11	0.01	0.11	0.11	0.09	0.07	0.03
NiO	0.07	0.00	0.08	0.08	0.09	0.06	0.23	0.18	0.13
MgO	17.7	18.9	17.4	18.0	17.3	17.1	18.9	17.9	18.9
CaO	16.6	21.4	17.3	21.4	17.5	17.1	21.2	23.4	20.6
Na_2O	1.23	0.47	1.10	0.23	0.92	1.35	0.27	<0.02	0.55
Total	100.52	100.74	99.99	100.00	100.11	100.00	100.10	100.07	100.03
mg	89.7	93.4	89.8	92.4	87	88.2	93.3	94.3	93.4

s secondary clinopyroxene in interstitial glass. *Total Fe as FeO; # WDS analyses

Table 5. *WDS and EDS electron microprobe analyses of spinel in peridotitic xenoliths from Cape Verde Islands (in wt%)*

Sample	CV-1	CV-1	CV-4	CV-4	CV-5	CV-5	CV-6	CV-6	CV-7	CV-7
	#	#s		s	#	#s		s		s
TiO_2	<0.02	1.06	0.61	1.41	0.41	0.50	0.09	0.23	2.69	2.03
Al_2O_3	24.4	8.6	2.5	8.4	38.8	25.8	26.7	9.6	18.8	6.3
Cr_2O_3	46.0	60.6	64.8	59.1	27.3	44.1	43.1	61.5	37.5	58.3
$Fe_2O_3^*$	1.71	1.89	6.2	1.7	5.2	1.00	1.94	1.13	10.9	4.5
FeO	12.7	13.9	11.7	18.0	9.0	12.0	11.8	14.3	15.8	15.8
MnO	0.22	0.36	1.04	1.35	<0.02	0.73	0.54	1.18	0.56	1.66
NiO	0.07	0.19	0.17	0.20	0.24	0.41	0.43	0.34	0.39	0.36
MgO	15.3	12.9	13.1	9.9	19.2	15.2	15.4	11.8	13.4	11.1
Total	100.38	99.52	100.02	100.01	100.01	99.74	100.00	100.01	99.99	100.00
mg	68.2	62.5	65.0	51.3	79.2	69.3	68.8	57.9	60.2	55.6

Sample	CV-8	CV-17	CV-17	CV-37	CV-37	CV-55	CV-55	CV-69	CV-69
	#s	#	#s		s	#	#s		s
TiO_2	1.92	0.69	1.49	0.86	1.41	0.35	1.14	0.14	4.30
Al_2O_3	24.6	43.5	14.4	41.9	8.4	52.4	13.1	23.6	10.7
Cr_2O_3	41.9	21.5	54.7	20.3	59.1	12.0	56.5	44.4	52.3
$Fe_2O_3^*$	1.69	4.81	0.44	7.3	1.70	5.9	0.40	4.0	0.48
FeO	13.8	9.8	15.1	10.8	18.0	7.2	16.0	11.6	20.7
MnO	0.24	0.68	1.04	0.21	1.35	0.03	0.09	1.11	0.99
NiO	0.24	0.30	0.34	0.30	0.20	0.88	0.44	0.20	0.14
MgO	15.2	18.8	12.6	18.3	9.9	21.2	12.1	15.0	10.3
Total	99.48	100.01	100.00	100.00	100.01	100.00	99.77	100.01	100.00
mg	66.3	76.2	59.2	74.6	48.0	82.9	57.5	76.2	46.5

s secondary spinel in interstitial glass. *Ferric iron was calculated assuming ideal stoichiometry. #WDS analyses

glass fills the interstitial spaces. Compositions of phases from host melanephelinites are given in Table 8. Clinopyroxenes are represented by calcic varieties (> 23 wt% CaO) with high Al_2O_3 contents (7–10 wt%) and relatively low concentrations of Na_2O (0.4–0.5 wt%). Titanomagnetites contain 20–25 wt% TiO_2.

The chemical composition of the matrix (mixture of crystals and residual glass) between olivine phenocrysts was analyzed with the SEM by scanning the electron beam over relatively large areas. Their compositions are also given in Table 8.

Table 6. *Composition of interstitial glasses in peridotitic xenoliths from Cape Verde Islands (EDS analyses in wt.-% and normalised to 100%)*

Sample	CV-1	CV-4	CV-5	CV-5	CV-7	CV-8	CV-8	CV-17	CV-37	CV-55	CV-55	CV-69	CV-69
SiO_2	51.5	43.7	55.7	64.7	57.7	62.8	59.4	64.8	40.6	67.5	58.4	47.6	58.0
TiO_2	<0.1	2.6	0.3	0.5	1.0	0.3	0.4	0.9	0.2	0.7	1.6	0.3	0.4
Al_2O_3	5.5	10.1	14.6	17.6	16.0	21.1	17.5	17.5	17.7	16.4	23.4	8.7	18.9
Cr_2O_3	0.1	0.1	0.1	0.2	0.2	0	0.2	0.3	0.2	0.2	0.5	0.4	0.2
FeO*	9.4	4.1	1.1	0.5	1.8	0.3	1.7	0.6	7.0	0.7	0.4	9.6	1.1
MnO	0.1	<0.1	0.1	0.3	<0.1	<0.1	0.2	0.1	0.2	<0.1	<0.1	0.2	0.2
NiO	0.3	0.2	0.1	0.2	0.2	<0.1	0.1	0.5	0.3	0.9	0.5	0.4	0.1
MgO	32.6	34.8	15.4	0.6	4.3	<0.1	8.7	1.5	30.3	0.6	3.3	29.8	1.9
CaO	0.4	1.1	3.2	1.3	2.0	4.2	1.5	1.2	0.7	1.0	3.1	1.2	1.5
Na_2O	0.2	0.3	3.3	3.6	6.1	4.7	0.3	4.1	0.2	3.6	3.0	<0.1	6.7
K_2O	0.4	0.2	3.6	8.1	7.7	5.9	1.8	7.2	0.3	8.4	5.8	0.3	7.9
P_2O_5	n.a.	1.7	1.2	1.2	1.6	n.a.	n.a.	1.1	1.3	n.a.	n.a.	0.9	2.1
S	n.a.	0.5	0.5	0.3	0.7	n.a.	n.a.	0.1	0.5	n.a.	n.a.	0.3	0.5

* Total Fe as FeO. *n.a.* not analysed for

Discussion

1. Estimation of p-T-x conditions

Equilibration temperatures for the primary minerals of mantle xenoliths have been calculated on the basis of two new versions of pyroxene geothermometers proposed by *Brey* and *Köhler* (1990). We provisionally selected a pressure of 20 kbar for these calculations. For some samples the equilibration pressure was calculated utilizing the Ca-in-olivine geobarometer of *Köhler* and *Brey* (1990).

For the majority of lherzolites the temperatures calculated on the basis of the compositions of coexisting pyroxenes (comparison of enstatite activities – T(1)) and on CaO contents of orthopyroxenes (T(2)) are consistent within 50 °C, and they are above 1200 °C (Table 9). All harzburgites yield T(1) values below 1200 °C, and for three specimens (CV-69, CV-6 and CV-4), T(1) is significantly lower than T(2). Orthopyroxenes from these specimens are also unusual in having Al_2O_3 contents higher than coexisting primary clinopyroxenes. All these features probably reflect cooling from higher temperatures which is also confirmed by the presence of exsolution lamellae in orthopyroxenes (Fig. 1d).

Olivines and other primary minerals from four lherzolites (CV-5, CV-8, CV-17 and CV-55) and one harzburgite (CV-1) were analysed for their calcium contents. No zonal Ca distribution has been found in any of the samples. Pressure and temperature estimates based on the simultaneous application of the Ca- in- olivine geobarometer and two-pyroxene geothermometer (*Köhler* and *Brey*, 1990) for CV-55 and CV-5 lie in the stability field of the spinel lherzolite phase assemblage

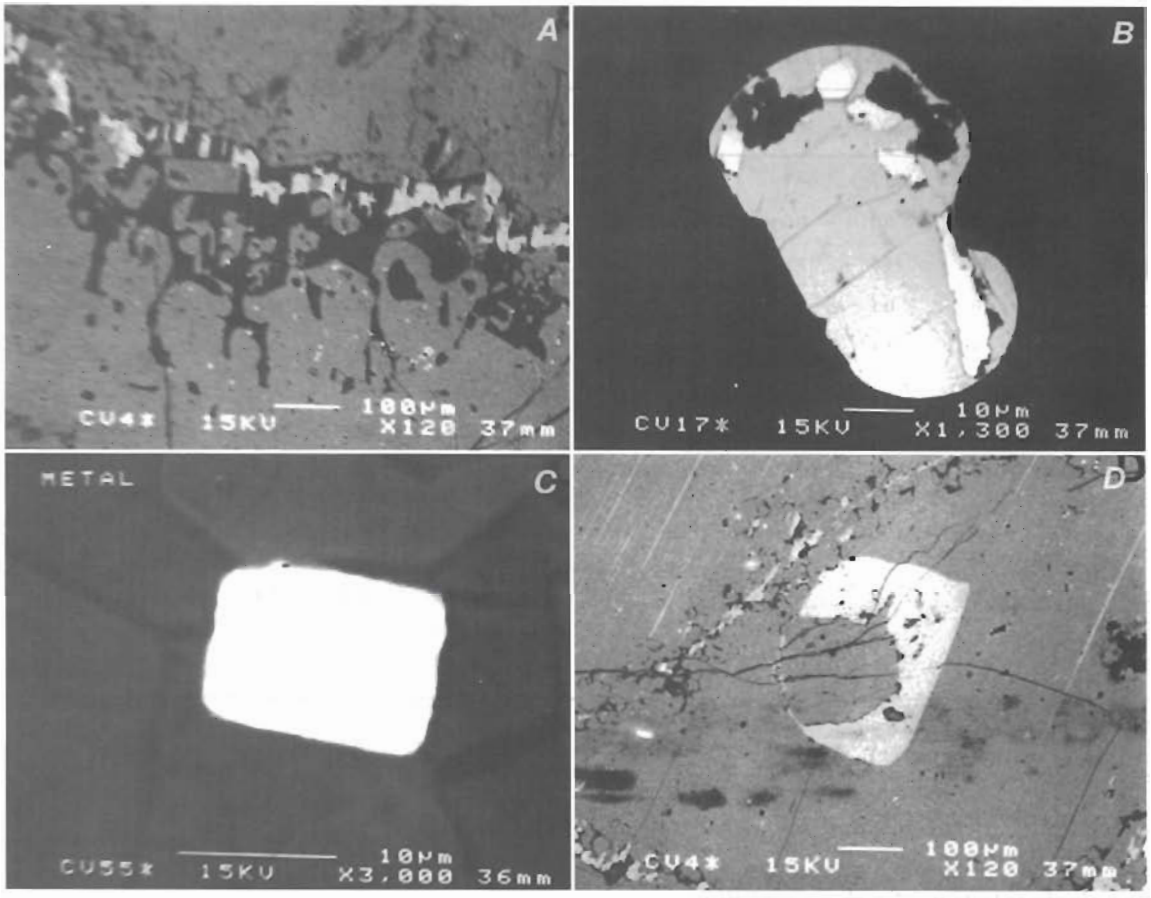

Fig. 1. **A** Veinlet of glass (the darkest phase) between two large grains of olivine. The glass includes small euhedral grains of olivine (grey) and clinopyroxene (the lightest phase). Sample CV-4, back-scattered electron image, length of bar is 100 µm. **B** Sulfide globule in glass with smaller segregations of metallic alloy (the lightest phase). Sample CV-17, back-scattered electron image, length of bar is 10 µm. **C** Euhedral crystal of Ni-Fe alloy in silicate glass touching a microphenocryst of clinopyroxene. Sample CV-55, back-scattered electron image, length of bar is 10 µm. **D** Clinopyroxene (light coloured phase) surrounding a small grain of olivine. Both are included in a large grain of orthopyroxene with thin exsolution lamellae. Pockets and veinlets of glass with microphenocrysts may be seen in various parts of this rock. Sample CV-4, back-scattered electron image, length of bar is 100 µm

according to *Webb* and *Wood* (1986). The p-T estimates for CV-17 fall very close to the phase boundary between spinel and garnet lherzolites (28.5 kbar for 1280 °C at $X_{Cr}^{Sp} = 0.25$, indistinguishable from our calculated pressure of 28.6 kbar within the error of the method). There is no primary spinel in sample CV-8 and we calculated the position of the garnet-in boundary for this specimen using garnet-orthopyroxene geobarometers. For this we have estimated the composition of garnet which may appear with increasing pressure in such a rock, using the experimental data on Mg-Fe exchange between olivine and garnet (*Brey* and *Köhler*, 1990) and the Ca content of lherzolitic garnets (*Brey*, unpublished Thesis, 1989). Estimates of p-T conditions based on this hypothetical garnet composition and the composition of orthopyroxene from CV-8 yields 30.3 kbar according to *Brey* and *Köhler's* (1990)

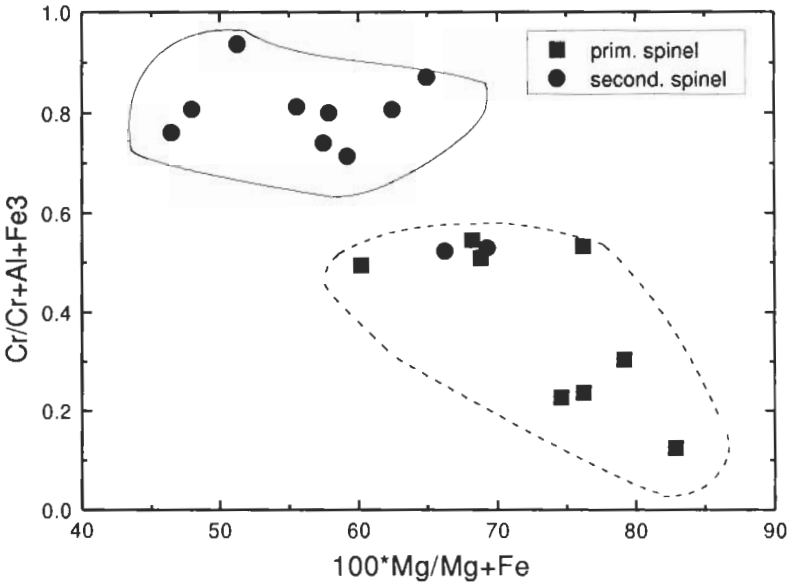

Fig. 2. Cation ratios in primary and secondary (reacted with melt) spinels

geobarometer, 30.6 kbar according to *Nickel* and *Green's* (1985) and 32.5 kbar according to *MacGregor's* (1974) method. Thus, comparison of the first two values with pressure estimated from CaO content in olivine (30.8 kbar) shows that we are very close to the garnet-in boundary while the third value would place this specimen outside the garnet lherzolite stability field. The absence of primary spinel in this specimen in addition to the fact that CV-8 is somewhat depleted, is obviously due to the high solubilities of Al_2O_3 and Cr_2O_3 in pyroxenes which in turn confirms the high temperature of equilibration provided by two-pyroxene thermometry. Estimated p and T for harzburgite CV-1 lie far from the garnet-in boundary and this probably holds also for other harzburgites. The fact that harzburgites are cooler than lherzolites appears to be in good agreement with the ideas of *Plank* and *Langmuir* (1992) in which the residual mantle column in a rising mantle diapir should be regularly stratified with increasing depletion upwards.

Oxygen fugacities for the primary mineral assemblages were calculated from the data on coexisting spinels, olivines and orthopyroxenes by the method described by *Wood* et al. (1990). These values are also given in Table 9. Oxygen fugacities range between −0.26 and +2.2 logarithmic units relative to the quartz-fayalite-magnetite (QFM) buffer. The average Δ QFM value is equal to 1.02. This result is consistent with the conclusion made by *Amundsen* and *Neumann* (1992) that the upper mantle beneath ocean islands is characterised by relatively high f_{O2}-values.

Interstitial melts record much lower f_{O2} values than the host peridotites as can be judged from the common occurrence of metallic alloys in the melts. As has been mentioned above, Ni-Fe solid solutions are particularly abundant in sample CV-55 where they also occur as isolated grains. Assuming that the metallic phase was in equilibrium with other microphenocrysts, and estimating the activity of Fe from the composition of Ni-Fe solid solution using *Fraser* and *Rammensee's* (1982) data, we calculated the f_{O2} from the equilibrium constant of the reaction $Fe + 1/2O_2 +$

Table 7. *Electron microprobe analyses of sulfides and metallic phases in peridotitic xenoliths from Cape Verde Islands (in wt.%)*

Sample	CV-1	CV-5	CV-5	CV-8	CV-8	CV-17	CV-17
Fe	20.5	98.5	19.0	27.9	32.4	42.8	35.9
Ni	45.8	0.70	52.7	63.2	28.0	54.7	32.7
Cu	<0.02	0.61	1.09	1.35	4.72	2.09	<0.02
S	33.5	0.17	27.3	0.86	34.3	0.37	31.4
Total	99.80	99.98	99.99	93.31	99.37	99.91	99.99

Sample	CV-37	CV-37	CV-55	CV-55	CV-69	CV-69
Fe	96.8	29.1	32.0	1.7	98.7	63.7
Ni	2.09	38.6	66.5	73.8	0.62	1.9
Cu	0.53	<0.02	1.29	<0.02	0.32	0.27
S	0.55	32.3	0.1	24.5	0.26	34.2
Total	99.99	99.94	99.90	99.94	99.90	100.06

$FeSiO_3 = Fe_2SiO_4$ which turns out to be 5 logarithmic units below QFM buffer. This estimate was based on the assumption that the microphenocryst assemblage is not far from equilibrium with orthopyroxene in spite of the fact that this mineral is not found among microphenocrysts. For these calculations we took the composition of orthopyroxene to be the same as that of the primary orthopyroxene from the same specimen.

Based on similar assumptions we may also estimate the oxygen fugacities for the microphenocryst assemblages of the intra-peridotite melt using the compositions of spinels. Oxygen fugacities calculated for spinel and olivine microphenocrysts taken together with primary orthopyroxene are in the majority of cases much lower than those calculated for primary mineral assemblages from the same nodules (the average values Δ QFM(2) in Table 9 is equal to -1.42). If we would introduce corrections for the lower $FeSiO_3$ activities (considering the absence of orthopyroxene microphenocrysts) the calculated f_{O2} values would be even lower. Thus, the

Table 8. *Composition of phenocrysts of olivine (Ol), clinopyroxene (Cpx), titanomagnetite (Sp) and matrices around olivine phenocrysts (GM) in melanephelinites (EDS analyses, recalculated and normalized)*

Sample	CV-17				Sample	CV-7		
Phase	GM	Cpx	Ol	Sp	GM	Cpx	Ol	Sp
SiO_2	40.7	45.3	40.1	<0.1	41.3	42.8	40.1	<0.1
TiO_2	4.1	3.6	0.2	20.4	4.0	4.4	0.1	24.4
Al_2O_3	10.3	7.0	0.5	4.6	11.3	9.9	1.0	3.4
Cr_2O_3	0.1	0.2	0.2	1.8	0.1	0.1	0.1	2.1
Fe_2O_3	1.2	5.2	<0.1	25.2	1.4	4.3	<0.1	17.4
FeO	5.6	1.2	12.7	41.4	8.0	2.9	13.1	46.3
MnO	0.2	<0.1	0.4	<0.1	0.2	0.1	0.2	1.3
NiO	0.2	0.2	0.5	0.6	0.1	0.2	0.2	0.2
MgO	9.7	13.0	44.4	6.1	10.3	11.6	44.0	5.0
CaO	20.1	24.0	1.0	<0.1	17.4	23.5	1.2	<0.1
Na_2O	3.0	0.5	<0.1	<0.1	2.7	0.4	<0.1	<0.1
K_2O	1.2	<0.1	<0.1	<0.1	1.3	<0.1	<0.1	<0.1
P_2O_5	3.5	<0.1	<0.1	<0.1	1.7	<0.1	<0.1	<0.1
S	0.2	<0.1	<0.1	<0.1	0.3	<0.1	<0.1	<0.1
Total	100.1	100.2	100.0	100.1	100.1	100.2	100.0	100.1

Note: ferric and ferrous iron were calculated for clinopyroxenes and titanomagnetites assuming ideal stoichiometry of these phases; in hypothetical melts represented by matrices between olivines. Fe^{2+} and Fe^{3+} were calculated using *Kilinc*'s et al. (1983) formula and estimated f_{O_2} values given in Table 9 (Δ QFM(3))

reduced character of spinels from interstitial peridotitic glasses is consistent with the presence of metallic phases.

In the host melanephelinites clinopyroxene and titanomagnetite started to precipitate after the crystallization of olivine phenocrysts. In order to estimate the temperature of equilibrium between these three minerals we used the compositions of the matrix surrounding the olivine phenocrysts given in Table 8. These compositions and the MgO contents of olivines permitted the calculation of the equilibrium temperature between olivine and melt using the formula of *Roeder* and *Emslie* (1970). Thus, temperature estimates range from 1230 to 1250 °C for three samples (T(4) in Table 9). They are consistent with the measurements of homogenization temperature (1200–1230 °C) for melt microinclusions in olivine from one of the melanephelinites from Sal Island (*Kogarko*, 1990).

We also made an attempt to estimate the f_{O_2} recorded by the equilibrium between titanomagnetite, olivine, clinopyroxene and liquid during the crystallization

Table 9. *Temperatures and oxygen fugacities estimated for the mineral assemblages of peridotitic xenoliths and melt pockets within them from Cape Verde Islands*

Sample	T(1) °C	P,kb	T(2) °C	Δ QFM(1)	T(3) °C	Δ QFM(2)	T(4) °C	Δ QFM(3)
CV-1	949	20.7	984	-0.60	>1112	<-1.27		
CV-4	755		1163	2.2	>1153	< 0.36	1252	1.69(1.36)
CV-5	1248	21.8	1220	1.01	>1164	<-1.61		
CV-6	1135		1205	-0.26	>1184	<-0.99		
CV-7	1211		1197	1.98	>1175	< 0.66	1252	1.01(0.68)
CV-8	1306	30.8	1288		>1094	<-1.16		
CV-17	1278	28.6	1258	0.79	>1084	<-3.14	1234	1.55(1.27)
CV-37	1244		1172	0.59	>1086	<-1.91		
CV-55	1251	19.6	1207	0.89	>1098	<-2.96		
CV-69	953		1228	0.96	>1130	<-3.06		

Note: T(1) and T(2) are temperatures of two pyroxene equilibria for primary peridotitic mineral assemblages calculated by formulae (9) and (10) of *Brey* and *Köhler* (1990), respectively; P are pressures estimated by the method of *Köhler* and *Brey* (1990) for specimens where Ca in olivine was analyzed following the recommendations of *Köhler* and *Brey*; for the rest of specimens T(1) and T(2) were estimated at P = 20 kb; T(3) is calculated by formula (9) of *Brey* and *Köhler* (1990) for clinopyroxene microphenocrysts from the interstitial peridotitic glasses under the assumption of their equilibration with primary orthopyroxenes from the same specimens; T(4) is a temperature calculated by the method of *Roeder* and *Emslie* (1970) from the compositions of olivine phenocrysts and matrices between them from the host melanephelinites; Δ QFM(1) are logarithms of oxygen fugacities normalized to QFM buffer calculated for the Sp + Ol + Opx assemblages of primary peridotitic minerals by the equation of *Wood* et al. (1990); Δ QFM(2) are similar values calculated for the assemblages of spinel and olivine microphenocrysts from peridotitic glasses under the assumption of their equilibration with primary orthopyroxenes from the same specimens; Δ QFM(3) are $\log_{10}(f_{O2}/f_{QFM})$ values calculated for titanomagnetite + olivine + clinopyroxene + melt equilibria in melanephelinites by the method described in text: first values calculated using parameters fitted from experimental data for high-Ca clinopyroxene + orthopyroxene + melt and values in brackets are based on experimental data for equilibria high-Ca clinopyroxene + low-Ca clinopyroxene + melt (list of publications is given in Appendix)

of the basaltic host magma. We based our calculations on the redox reaction for the QFM oxygen buffer. In order to estimate a_{SiO_2} we calculated a_{MgSiO_3} from the equilibrium constant (K) of the following exchange reaction

$$Mg_2Si_2O_6{}^{Opx} + CaO^L = CaMgSi_2O_6{}^{CPx} + MgO^L$$

which was regressed as a function of temperature from the published experimental data (see list of references in Appendix). The activity of enstatite was subsequently calculated as

$$a_{Mg2Si2O6} = K^* a_{CaMgSi2O6}/(Ca^L/Mg^L)$$

where $a_{CaMgSi2O6}$ was estimated from the composition of clinopyroxene and Ca^L/Mg^L is the ratio for the coexisting melt.

After this, a_{SiO2} was estimated from the reaction $Mg_2Si_2O_6 = Mg_2SiO_4 + SiO_2$, and f_{O2} was calculated by substitution of this value and also of activities of fayalite and Fe_3O_4 into the reaction constant of the QFM buffer. The last two values were estimated on the basis of olivine and titanomagnetite analyses using formulae published by *Ghiorso* and *Sack* (1991) and by *Wiser* and *Wood* (1991). These calculations yielded f_{O2} levels 0.8–1.5 log units above QFM (ΔQFM(3) values in Table 9).

2. *Mantle plume beneath Cape Verde*

The investigated peridotites belong to two groups: lherzolites, moderately depleted in magmaphile elements, and highly depleted harzburgites. Estimated equilibrium temperatures (T(1) values) given in Table 9 show that, judging from clinopyroxene compositions, lherzolites equilibrated at higher temperatures than harzburgites. Assuming that temperature increases with depth, we may conclude, that the mantle underneath Cape Verde is stratified with harzburgites concentrated in the upper part. This is consistent with the model of oceanic lithosphere suggested by *Plank* and *Langmuir* (1992). These authors maintain that the residual mantle column resulting from the partial melting of rising plumes should have peridotites, which are more depleted with respect to magmaphile elements (harzburgites or dunites), lying above more fertile lherzolites. Cape Verde is a well known oceanic swell. Bathymetric, gravity and temperature anomalies across the Cape Verde swell are typical evidences for a mantle plume (*Courtney* and *White*, 1986).

Unfortunately, estimated pressures do not permit us to test this conclusion because of the wide uncertainty range especially for harzburgitic phase assemblages: slight variations of estimated temperatures cause calculated pressure to vary considerably. The value of 20.7 kbar obtained for harzburgite CV-1 is in the range of lower estimates for lherzolitic phase assemblages. Considering the indications of cooling effects reflected in the compositions of orthopyroxenes from some harzburgites (relatively high CaO and Al_2O_3 contents) we may suspect that the Ca content in olivine may correspond to a temperature lower than that estimated from the two-pyroxene geothermometer, and, therefore, it would imply a pressure lower than 20 kbar.

3. *The origin of interstitial glass, sulfides and metallic phases*

Interstitial glasses in Cape Verde peridotites are highly variable in their composition. Some of them may represent melts formed in situ during eruption, others (highly potassic varieties) require a pre-melting metasomatic enrichment. A distinctive feature of these melts is their very low redox potential manifested in the presence of metallic phases and low Fe^{3+} contents of secondary spinels. Temperatures of at least some melts (MgO-rich varieties) must have been high, which is also reflected in

extraordinary high chromium contents in olivine microphenocrysts. For example, application of the *Roeder* and *Emslie* (1970) method to coexisting olivine and melt from specimen CV-1 gives a temperature around 1600 °C which is clearly too high and probably requires the participation of volatiles in the formation of interstitial melts. The presence of volatiles is corroborated by abundant fluid inclusions in the peridotite minerals.

The interstitial glasses in Cape Verde mantle xenoliths are in many respects similar to those described from other localities. The occurrence of Si-, Al-, Na- and K-rich glasses and their extreme variability in chemical composition were also reported for peridotitic xenoliths from Tahaa Island, Society Archipelago (*Schiano* et al., 1992), from Gees, West Eifel, Germany (*Edgar* et al., 1989) and from Lanzarote, Canary Islands (*Siena* et al., 1991). The maximum SiO_2 content of glasses from Gees is 63.34%, from Tahaa it is 65.06%, from Lanzarote 72.63% and from Cape Verde 67.54% (Table 6), for Al_2O_3 these values are 22.73, 18.48, 19.64%, and 23.4%, respectively, for Na_2O they are 5.94%, 6.1%, 5.27% and 6.7%, and for K_2O 8.29%, 10.43%, 2.85% and 8.4% respectively. Similar to other localities, the glasses in the Cape Verde peridotites drastically differ in their composition from that of the host melanephelinitic lavas. This contrast is further enhanced by the large differences in oxygen fugacities between these two types of melts (see Table 9). Such differences effectively rule out a common origin of the melt in the xenolith and the host nephelinitic lavas.

According to a very popular hypothesis, interstitial glasses are produced from volatile-rich melts which percolated at depth through the mantle rocks and were responsible for their metasomatic alterations (*Edgar* et al., 1989; *Schiano* et al., 1992). Equilibrium temperatures of primary minerals estimated by us for the Cape Verde lherzolites are indeed very high, and they are undoubtedly well above the solidi of peridotite-CO_2 and peridotite-H_2O systems. It is, therefore, very likely that small amounts of intergranular melt were present in these rocks at depth, and this melt might have concentrated potassium and other incompatible elements. However, compositions of these melts must have changed during the eruption due to the interaction with minerals of the peridotite at low pressure and also due to the mixing with a liquid, which might have been formed by additional melting of rock-forming minerals caused by heating by the host magma and by decompression. These non-equilibrium processes were likely to have been responsible for the variability of glass composition within a given xenolith.

Sulfide globules were described in detail by *MacRae* (1979) in interstitial glass of ultramafic xenoliths from the Tertiary Newer Basalts of Victoria, Australia. However, in contrast to sulfides in Cape Verde peridotites these globules from Victoria contain Fe-oxides which clearly reflect more oxidizing conditions as compared to Cape Verde. *MacRae* (1979) suggests that these sulfides formed due to the interaction of a gas phase liberated from the host basanite magma during its ascent with the ultramafic xenoliths. In the case of Cape Verde xenoliths such an explanation does not seem very plausible, because the host basaltoid magma and the gas, which may separate from it, are characterized by relatively high oxygen fugacities and, therefore, such vapour may not produce strongly reduced metal-bearing sulfide aggregates. It is more likely that the sulfide phases were present at depth between the grains of major minerals of peridotites, as is commonly observed in peridotitic xenoliths (e.g.,

Ionov et al., 1992). Many of the Cape Verde Island xenoliths are characterized by high mineral equilibration temperatures (above 1250 °C) which are above the liquidi of sulfides (*Boehler*, 1992). It is therefore likely that the sulfides were present in these rocks as liquid droplets immiscible with the interstitial silicate melt. It can also not be excluded that in some cases (particularly for lherzolite CV-37, anomalously rich in sulfide and metallic phases) sulfides were introduced into mantle rocks by percolating melts, as it has been suggested for orogenic peridotites by *Lorand* (1991) or by fluids which could have condensed liquid sulfides into intergranular space. Sulfur might have been dissolved in silicate melt and the exsolution of sulfide liquid could have been caused by the precipitation of microphenocrysts.

In the upper mantle, sulfides must have been in equilibrium with the primary mineral assemblages characterized by relatively high f_{O2}-values (Table 9), which precluded formation of metallic alloys at depth. Metallic phases probably formed during the eruption when decompression might have resulted in the desulfurization of sulfides by the reactions of the following types:

$$FeS + 3Fe_2O_3{}^L = 7FeO^L + SO_2{}^G$$

$$FeS + 2FeO^L = 3Fe^{met} + SO_2{}^G$$

As a result of these processes, metallic phases formed and a dramatic reduction in oxygen fugacity in the local system occupying the intergranular space of the peridotite nodules took place. This strongly reduced environment is reflected not only in the presence of metallic grains and low-sulfur sulfides (such as $Ni_{3+x}S_2$ phase) in the interstitial glasses, but also in the very low ferric iron contents of spinel microphenocrysts.

In contrast to the mineral assemblages of interstitial glasses, oxygen fugacities recorded by the compositions of primary minerals of the investigated spinel peridotites are much higher and comparable with the f_{O2} values estimated for the host nephelinitic magma. In principle, such melts could have been produced by low degrees of partial melting of peridotites similar to those represented by the investigated nodules. The presence of K-rich material introduced into these peridotites by a metasomatic event, similar to that invoked here to explain the formation of K-rich peridotitic glasses, might have also been important for the generation of basaltic melts at deeper levels in the mantle.

Conclusions

1. Mantle xenoliths from the Sal Island, Cape Verde Archipelago, comprise refractory harzburgites and moderately depleted lherzolites. The lherzolites have high (> 1250 °C) equilibration temperatures which contrast with those of the harzburgites (T < 1000 °C). This may reflect the presence of a hot asthenospheric diapir underneath a cool refractory lithosphere.
2. T-p estimates for some of the investigated lherzolites place them close to the upper boundary of the garnet lherzolite facies.
3. Metallic phases (Ni-Fe-Cu alloys), often associated with sulfides, are present in the interstitial glasses of mantle peridotite xenoliths. They probably formed by desulfurization of sulfides during ascent of xenoliths with the melanephelinitic host.

4. Very low f_{O2} values have been determined for the interstitial melts. They are reflected by the presence of metallic alloys and of low-S sulfides, and by low contents of Fe^{3+} in secondary spinels.
5. The f_{O2} values inferred for primary mineral assemblages of the peridotites are much higher than those for intergranular melts, and they are comparable to oxygen fugacities estimated for the host basaltic rocks.
6. High temperatures (above 1250 °C) estimated for the primary mineral equilibria for lherzolites imply that at depth these rocks have probably contained intergranular volatile-rich silicate melt, rich in K_2O and other incompatible elements and droplets of immiscible sulfide liquid.
7. Highly magnesian glasses with low alkali contents could be the product of in situ melting during volcanic eruption.

Acknowledgements

This work has been partly supported by the Fund of Fundamental Studies of the Russian Federation (grants 93-05-14538 and 93-05-8463). The Austrian Academy of Sciences and the University of Vienna financed visits of IDR to Austria, and this made possible this joint research. The authors are indebted to Dr. *F. Brandstätter* for his help with the work on the SEM, and to Dr. *G. Brey* for his review.

References

Amundsen HEF, Neumann E-R (1992) Redox control during mantle/melt interaction. Geochim Cosmochim Acta 56: 2405–2416

Armstrong JT (1988) Quantitative analysis of silicate and oxide materials: comparison of Monte Carlo, ZAF, and $\phi(\rho z)$ procedures. In: Newbury DE (ed) Microbeam analysis. San Francisco Press, pp 239–246

Boehler R (1992) Melting of the Fe-FeO and Fe-FeS systems at high pressure: constraints on core temperatures. Earth Planet Sci Lett 111: 217–227

Brey GP, Köhler T (1990) Geothermobarometry in four-phase lherzolites. II. New thermobarometers, and practical assessment of existing thermobarometers. Geochim Cosmochim Acta 31: 1353–1378

Caperdi S, Venturelli G, Salvioli-Mariani E, Crawford AJ, Barbieri M (1989) Upper mantle xenoliths and megacrysts in an alkali basalt from Tallante, South-eastern Spain. Eur J Mineral 1: 685–699

Courtney RC, White RS (1986) Anomalous heat flow and geoid across the Cape Verde Rise: evidence for dynamic support from a thermal plume in the mantle. Geophys J R Astron Soc 87: 815–867

De Paepe P, Klerx J (1971) Peridotite nodules in nephelinites from Sal (Cape Verde Islands). Ann Soc Geol Belgique 41: 311–316

Edgar AD, Llyod FE, Forsyth DM, Barnett RL (1989) Origin of glass in upper mantle xenoliths from the quarternary volcanics of Gees, west Eifel, Germany. Contrib Mineral Petrol 103: 277–286

Ellis DJ (1976) High pressure cognate inclusions in the Newer Volcanics of Victoria. Contrib Mineral Petrol 58: 149–180

Elthon D, Scarfe CM (1984) High-pressure phase equilibria of a high-magnesia basalt and the genesis of primary oceanic basalts. Am Mineral 69: 1–15

Falloon TJ, Green DH (1987) Anhydrous partial melting of MORB pyrolite and other peridotite compositions at 10 kbar: implications for the origin of primitive MORB glasses. Mineral Petrol 37: 181–219

Francis D (1991) Some implications of xenolith glasses for the mantle sources of alkaline mafic magmas. Contrib Mineral Petrol 108: 175–180

Fraser DG, Rammensee W (1982) Activity mesurements by Knudsen cell mass spectrometry – the system Fe-Co-Ni and implications for condensation processes in the solar nebula. Geochim Cosmochim Acta 46: 549–556

Frey FA, Green DH (1974) The mineralogy, geochemistry, and origin of lherzolite inclusions in Victorian basanites. Geochim Cosmochim Acta 49: 1023–1059

Fujii T, Bougault H (1983) Melting relations of a magnesian abyssal tholeiite and the origin of MORBs. Earth Planet Sci Lett 62: 283–295

Gamble JA, Kyle PR (1987) The origin of glass and amphibole in spinel-wehrlite xenoliths from Foster Crater, McMurdo volcanic group, Antarctica. J Petrol 28: 755–779

Garcia MO, Presti AA (1987) Glass in garnet pyroxenite xenoliths from Kaula Island, Hawaii: product of infiltration of host nephelinite. Geology 15: 904–906

Ghiorso MS, Sack RO (1991) Fe-Ti oxide geothermometry: thermodynamic formulation and the estimation of intensive variables in silicic magmas. Contrib Mineral Petrol 108: 485–510

Girnis AV, Ryabchikov ID, Bogatikov OA (1987) Genesis of komatiites and komatiitic basalts (in Russian). Nauka, Moscow, 120 p

Grove TL, Bryan WB (1983) Fractionation of pyroxene-phyric MORB at low pressure: an experimental study. Contrib Mineral Petrol 84: 293–309

Grove TL, Juster TC (1989) Experimental investigations of low-Ca pyroxene stability and the pyroxene-liquid equilibria at 1 atm in natural basaltic and andesitic liquids. Contrib Mineral Petrol 103: 287–305

Grove TL, Gerlach DC, Sando TW (1982) Origin of calc-alkaline series lavas at Medicine lake volcano by fractionation, assimilation and mixing. Contrib Mineral Petrol 80: 160–182

Ionov DA, Hoefs J, Wedepohl KH, Wiechert U (1992) Content and isotopic composition of sulphur in ultramafic xenoliths from Central Asia. Earth Planet Sci Lett 111: 269–286

Juster TC, Grove TL, Perfit MR (1989) Experimental constraints on the generation of FeTi basalts, andesites and rhyodacites at the Galapagos spreading center 85 W and 95 W. J Geophys Res 4: 9251–9274

Kilinc A, Carmichael ISE, Rivers ML, Sack RO (1983) The ferric-ferrous ratio of natural silicate liquids equilibrated in air. Contrib Mineral Petrol 83: 136–140

Kleeman JD, Green DH, Lovering JF (1969) Uranium distribution in ultramafic inclusions from Victorian Basalts. Earth Planet Sci Lett 5: 449–458

Kogarko LN (1990) Geochemistry of magmatic rocks. In: *Pushcharovsky YuM* (ed) Tectonics and magmatism of Cape Verde Islands (in Russian). Nauka, Moscow, pp 157–207

Köhler TP, Brey GP (1990) Calcium exchange between olivine and clinopyroxene calibrated as geothermobarometer for natural peridotites from 2 to 60 kb with applications. Geochim Cosmochim Acta 54: 2375–2388

Kuo LC, Essene EJ (1986) Petrology of spinel harzburgite xenoliths from the Kishb Plateau, Saudi Arabia. Contrib Mineral Petrol 93: 335–346

Longhi J (1987) Liquidus equilibria and solid solution in the system $CaAl_2Si_2O_8$-Mg_2SiO_4-$CaSiO_3$-SiO_2 at low pressure. Am J Sci 287: 265–331

Longhi J, Pan V (1988) A reconnaisance study of phase boundaries in low-alkali basaltic liquids. J Petrol 29: 115–147

Lorand J-P (1991) Sulphide petrology and sulphur geochemistry of orogenic lherzolites: a comparative study of the Pyrenean bodies (France) and Lanzo Massif (Italy). J Petrol (Special Volume "Orogenic Lherzolites and Mantle Processes"): 77–95

MacGregor ID (1974) The system MgO-Al_2O_3-SiO_2: solubility of Al_2O_3 in enstatite for spinel and garnet peridotite compositions. Am Mineral 59: 110–119

MacRae ND (1979) Silicate glass and sulphides in ultramafic xenoliths, Newer Basalts, Victoria, Australia. Contrib Mineral Petrol 68: 275–280

Mendes MH, Silva LC (1983) Preliminary note on the occurrence of peridotite nodules in Santiago (Cape Verde Islands). Garcia de Orta, Ser Geol 6: 1–2

Mercier JC, Nicolas A (1975) Textures and fabrics of upper mantle peridotites as illustrated by basalt xenoliths. J Petrol 16: 454–487

Meen JK (1990) Elevation of potassium content of basaltic magma by fractional crystallization: the effect of pressure. Contrib Mineral Petrol 104: 309–331

Nickel K, Green DH (1985) Empirical geothermobarometry for garnet peridotites and implications for the nature of the lithosphere, kimberlites and diamonds. Earth Planet Sci Lett 73: 158–170

Nielsen RL, Davidson PM, Grove TL (1988) Pyroxene-melt equilibria: an updated model. Contrib Mineral Petrol 100: 361–373

Plank T, Langmuir HC (1992) Effects of the melting regime on the composition of the oceanic crust. J Geophys Res 97: 19749–19770

Rhodes JM, Lofgren GE, Smith DP (1979) One atmosphere melting experiments on ilmenite basalt 12008. Proc Lunar Planet Sci Conf 10th: 407–422

Roeder PL, Emslie RF (1970) Olivine-liquid equilibrium. Contrib Mineral Petrol 29: 275–289

Sack RO, Carmichael ISE (1984) Fe2 = Mg2 and TiAl2 = MgSi2 exchange reactions between clinopyroxenes and silicate melts. Contrib Mineral Petrol 85: 103–115

Schiano P, Clocchiatti R, Joron JL (1992) Melt and fluid inclusions in basalts and xenoliths from Tahaa Island, Society archipelago: evidence for a metasomatized upper mantle. Earth Planet Sci Lett 111: 69–82

Siena F, Coltori M (1993) Thermobarometric evolution and metasomatic processes of upper mantle in different tectonic settings: evidence from spinel peridotite xenoliths. Eur J Mineral 5: 1073–1090

Siena F, Beccaluva L, Coltorti M, Marchesi S, Morra V (1991) Ridge to hot-spot evolution of the Atlantic lithospheric mantle: evidence from Lanzarote peridotite xenoliths (Canary Islands). J Petrol (Special Volume "Orogenic lherzolites and mantle processes"): 271–290

Takahashi E, Kushiro I (1983) Melting of a dry peridotite at high pressure and basalt magma genesis. Am Mineral 68: 859–879

Tatsumi Y, Sakuyama M, Fukuyama H, Kushiro I (1983) Generation of arc basalt magmas and thermal structure of the mantle wedge in subduction zones. J Geophys Res 88: 5815–5825

Wiser NM, Wood BJ (1991) Experimental determination of activities in Fe-Mg olivine at 1400 K. Contrib Mineral Petrol 108: 146–153

Webb SAC, Wood BJ (1986) Spinel-pyroxene-garnet relationships and their dependence on Cr/Al ratio. Contrib Mineral Petrol 92: 471–480

Wood BJ, Bryndzia LT, Johnsen KE (1990) Mantle oxidation state and its relationship to tectonic environment and fluid speciation. Science 248: 337–345

Authors' addresses: Prof. Dr. *J. D. Ryabchikov*, Institute for Geology of Ore Deposits, Russian Academy of Sciences, Moscow 109017, Russia; Dr. *T. Ntaflos*, Universität Wien-Geozentrum, Institut für Petrologie, Althanstrasse 14, A-1090 Wien, Austria; Prof.

Dr. *G. Kurat*, Naturhistorisches Museum, Wien, Burgring 7, A-1010 Wien, Austria; Prof. Dr. *L. N. Kogarko*, Vernadsky Institute of Geochemistry, Russian Academy of Sciences, Moscow 117975, Russia.

Appendix

Experimental data for two pyroxene + melt equilibria were taken from the following publications:

Elthon D, Scarfe CM (1984)
Falloon TJ, Green DH (1987)
Fujii T, Bougault H (1983)
Girnis AV, Ryabchikov ID, Bogatikov OA (1987)
Grove TL, Bryan WB (1983)
Grove TL, Gerlach DC, Sando TW (1982)
Grove TL, Juster TC (1989)
Juster TC, Grove TL, Perfit MR (1989)
Longhi J (1987)
Longhi J, Pan V (1988)
Meen JK (1990)
Nielsen RL, Davidson PM, Grove TL (1988)
Rhodes JM, Lofgren GE, Smith DP (1979)
Sack RO, Carmichael ISE (1984)
Takahashi E (1986)
Tatsumi Y, Sakuyama M, Fukuyama H, Kushiro I (1983)